

Chapter 1

Introduction

1-1 An overview of low temperature poly-silicon(LTPS)

Low temperature polysilicon crystallization for producing large-grained polycrystalline Si films on high temperature incompatible amorphous substrates have been studied extensively in the past decade [1-2]. These materials are important for integration of driver circuitry into large-area microelectronics in applications such as active matrix liquid crystal displays (AMLCD) or organic light-emitting diodes (OLEDs) that reside on substrate such as glass or plastic. High performance thin-film transistor (TFT) device fabricated using these materials for the active region are desirable, as they can enable integration of various driver components directly onto the substrate in order to reduce manufacturing costs, and to increase the functionality of large-area microelectronics. Techniques of crystallizing a semiconductor film formed on an insulating substrate such as glass and techniques of increasing crystalline thereof by using laser annealing have been researched widely in recent years. Because of the glass substrates have the advantage of low cost, good workability, and the easy with the large area substrate can be made than quartz substrates. The reasons that lasers are preferably used in crystallization are that the glass substrate melting point is low, and it is necessary to reduce the processing temperature to a temperature less than 600°C. Lasers can impart high energy only to a semiconductor film without causing the substrate temperature to increase very much. And crystalline semiconductor films formed by laser crystallization have high mobility, and thin film transistors are formed using the crystalline semiconductor

films. Both of them were why most of research utilized the LTPS techniques.

Some method of laser crystallization liked the excimer laser crystallization (ELA), solid state laser (SSL), sequential lateral solidification (SLS), and metal induced lateral crystallization (MILC) have been application for LTPS.

1-1-1 Comparison of SSL and Excimer laser

Excimer laser have a short pulse length (15-50ns),and the short optical adsorption depth (308nm). Compared to the solid state laser, solid state laser are maintenance-free, have stable output, and are superior to excimer lasers in mass production because it is possible to have higher repetitive oscillation when using a solid laser as a pulse laser than when using an excimer laser. However there are not many types of solid lasers, and almost all available solid lasers have an oscillation wavelength (fundamental wave) in the red color region or the infrared region. Semiconductor films absorb almost no light in the red color or infrared region, and therefore the second harmonic (2ω) or the third harmonic (3ω) corresponding to a wavelength in the range of the visible light region to the ultraviolet light region is used when a solid laser is utilized during laser crystallization. A stable diode pumped solid state laser (DPSS) was used to form poly-Si on a glass substrate .The power stability of the DPSS CW laser is less than 1%, which value is superior to XeCl excimer laser. A technique of laser crystallization for forming a polycrystalline silicon film having a large grain size on a glass substrate using a CW Nd:YVO₄ laser with laser diode (LD) excitation has been developed recently. It is possible to manufacture TFT with the mobility greater than 600 ($cm^2/V-s$) [3].

1-2 Photo leakage current of Poly-Si TFTs

Poly-Si TFTs are widely used in active-matrix liquid crystal displays (AMLCD) . It will be influenced by the backlight, and then create the photo leakage current. The photo leakage results in the decrease of pixel voltage and the increase of the cross talk. So the suppression of photo leakage current has been an important issue in the fabrication of high-brightness liquid-crystal projectors. Some of the method to suppress the photo current was to use the LDD structure and hydrogenated. It is found that photo leakage current is mainly generated at the offset region and the decrease in the offset length .This is because the electric field is applied to the offset region and carriers generated in the region [4-5]. It is well known that a large number of traps exist in the grain boundaries, the interface between the gate oxide and the poly-Si channel causing a large leakage current. However the traps should be suppressed by the hydrogenation process for real applications. In addition, the reduction of traps will enhance the photo excited current under an illuminated environment [6]. Hence, suppressing the photo excited current and keeping the low dark-current for hydrogenated TFTs under illumination is very important. Combined the hydrogenation and oxidation process method will decrease the dark current and photo current. In addition, the on current is improved and subthreshold swing is better [7]. The other author developed an LTPS LCLV(Liquid Crystal Light Valve) with a light-shielding structure, where an additional light absorptive shielding layer is placed between the active layer of the TFT and the lower light-shielding layer. This light absorptive shielding layer effectively blocks any incident light that might enter the space near the TFT active layer from the side of light-shielding layers, preventing the weaker light from reaching the TFT active layer [8].

1-3 Motivation

As mentioned in 1-2, high illumination intensity increases the photo leakage current of Poly-Si TFTs, and results in the decrease of pixel voltage and increase of the cross talk. Recent study indicate that the photo leakage current of Poly-Si TFTs that is generated in the depletion region near the drain side. As the development of color sequential technology, the backlight of Red 、 Green 、 Blue color will be irradiated in order. Under higher illumination, photo leakage current in the poly-Si TFTs with the illumination of RGB color haven't been discussed. The purpose of research topic is to discuss the devices photo leakage current of Poly-Si TFTs in the panel of RGB sub-pixel. It is expected that the light of blue color has the larger leakage current because color of blue light has the larger absorption coefficient.

1-4 Thesis Outline

This thesis is organized into the following chapters:

In the chapter 1, a brief overview of thin-film transistor is introduced to describe the various applications. Then the meaning of photo leakage current is discussed.

In the chapter2, the process flow of poly-Si films with different conditions is introduced. We study the crystallization mechanism of a-Si annealed by high-power Nd:YAG laser beam with 532-*nm* wavelength. Devices with various poly-Si film conditions are also characterized and directly related to the thin film material properties. We measured activation energy with different bias under different film quality, and studied the trap density with various grain sizes.

In the chapter 3, we studied the influence of photo leakage current .The dependence of photo leakage current on channel width and channel length; lightly drain doping (LDD) length, channel thickness and grain size are characterized. And the devices

photo leakage current of Poly-Si TFTs in the panel of RGB sub-pixel is also investigated. It is expected that the light of blue color has the larger photo leakage current because color of blue light has the larger absorption coefficient.

In the chapter4, the results of our experiments and analysis are concluded.



Chapter 2

Analysis of Activation Energy for Poly-Si TFTs

2-1. Device fabrication and measurement

Device fabrication

The figure 2-1 shows the cross-sectional view of standard top-gate poly-Si TFT with overlap LDD. These devices were fabricated on glass substrate with the buffer layer of the silicon nitride 50nm , silicon oxide 100nm , then followed by the deposition a-Si film by plasma enhanced chemical vapor deposition (PECVD). After the device islands were defined, a 100nm gate oxide was deposited by PECVD. Finally, the metal gate electrode was deposited and patterned. In this paper, we use two groups of devices. The first-group devices, the a-Si film are utilizing the solid state laser to crystallize the amorphous films to poly-Si film. The a-Si film was irradiated by the solid-state laser with laser energy density varies from 369 mJ/cm^2 to 645 mJ/cm^2 to form the various dimension of grain size. And the channel thickness of poly-Si film was 50nm , 75nm , and 100nm . The second-group devices, the a-Si film are utilizing the Excimer laser annealing to crystallize the amorphous films to poly-Si film. And only one condition of grain size was used, the channel thickness was 50 nm .

The device channel length varies from $6\mu\text{m}$ to $30\mu\text{m}$ when the channel is fixed as $6,30\mu\text{m}$. And lightly drain doping (LDD) length is various by $1\mu\text{m}$ to $3\mu\text{m}$.

Measurement

The current-voltage characteristic measurement of thin film transistor devices was performed by HP4156A semiconductor parameter analyzer with source grounded. Photo leakage current have been measured in standard top gate overlap poly-Si TFTs

with back face illumination, the light source was Cold Cathode Fluorescent (CCFL) backlight. Light luminance of CCFL was control by the Programmable Power Supply PPT-3615G, it was measured by the instrument of Conoscope. About the photo leakage current with the illumination of RGB color, the light of RGB color was used the filter above the CCFL back light. The color coordinate of RGB color was measurement utilizing the Conoscope. At the same time, the wavelength characteristics of Red, Green, Blue colors were measured by the spectrometer.

2-2. Methods of parameter extraction

In this section, we will introduce the methods of parameter extraction, included the threshold voltage (V_t), field effect mobility (μ), the trap state density (N_t), and grain barrier height (E_B). The current-voltage characteristic measurement of thin film transistor devices was performed by HP 4156A semiconductor parameter analyzer with source ground.

2-2-1. Determination of Threshold voltage

Many methods to determination the threshold voltage is the constant drain current method that the voltage at a specified drain current (threshold current I_N) is taken as the threshold voltage. This technique is adopted in most studies of TFTs. It can be give a threshold voltage close to that obtained by the complex linear extrapolation method. Typically, the threshold current $= I_D / (W_{eff} / L_{eff})$ is specified at 10 nA for $V_D = 0.1V$ and 100 nA for $V_D = 5V$ in most papers to extract the threshold voltage of TFTs.

2-2-2. Determination of Field effect mobility

The field effect mobility, μ_{FE} is determined from the transconductance, g_M at low

drain bias. The transfer characteristics of poly-Si TFTs are similar to those conventional single crystalline MOSFETs, so the first order I - V relation in the bulk Si MOSFETs can be applied to the poly-Si TFTs, which can be expressed as

$$I_D = C_{ox} \mu \frac{W}{L} (V_G - V_t) V_D - \frac{1}{2} V_D^2 \quad (2-2-1)$$

Where C_{ox} is the gate oxide capacitance per unit area, W , L represents the channel width and channel length, respectively, and V_t is the threshold voltage. If V_D is smaller than $V_G - V_t$, the drain current can be approximated as:

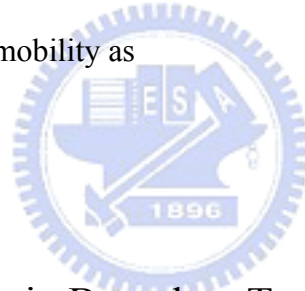
$$I_D = C_{ox} \mu \frac{W}{L} (V_G - V_t) V_D \quad (2-2-2)$$

The transconductance is defined by

$$g_M = C_{ox} \mu \frac{W}{L} V_D \quad (2-2-3)$$

We defined the field effect mobility as

$$\mu_{FE} = \frac{L}{W V_D C_{ox}} g_{M(\max)} \quad (2-2-4)$$



2-2-3. Extraction of Grain Boundary Trap State Density

The potential barrier created by the trapping states is related to the difference of the carrier concentrations between inside the grain and located on the grain boundaries. Based on this consideration, the amount of trap state density (N_t), may be extracted from the current-voltage characteristics of TFTs. We can simply estimate the value of N_t from the $\ln[I_D / (V_G - V_{fb}) V_D]$ versus $(V_G - V_{fb})^{-2}$ characteristics[9]. The details are as followed:

$$I_D = C_{ox} \frac{W}{L} (V_G - V_t) V_D \mu_B \exp\left(-\frac{qE_B}{KT}\right) \quad (2-2-5)$$

Where q is the electron charge.

K is the Boltzmann's constant

T is the channel thickness.

V_t is the threshold voltage.

$$E_B = \frac{q^2 N t^2}{8n\epsilon_{si}} = \frac{q^2 N t^2 t}{8C_{ox}(V_G - V_t)} \quad (2-2-6)$$

n is the gate induced free carrier concentration in the grains and is equal to $C_{ox}(V_G - V_t)/t$, ϵ_{si} is the dielectric constant. The channel thickness t_{ch} is defined as the thickness with 80% gate-induced carriers within [10] :

$$I_D = C_{ox} \frac{W}{L} (V_G - V_t) V_D \mu_B \exp\left(-\frac{q^2 N t^2 t_{ox}}{\sqrt{\epsilon_{si} \epsilon_{siO_2}} C_{ox} (V_G - V_T)^2}\right) \quad (2-2-7)$$

Accordingly, the effective trap state density can be obtained from the slope of the curve $\ln[I_D / (V_G - V_t)]$ versus $(V_G - V_t)^{-2}$

2-3 Material analysis

2-3-1 Scanning electron microscope (SEM)

By observing the SEM images of figure 2-3, the lateral growth was happened between the laser energy density of 553 mJ/cm^2 and 599 mJ/cm^2 in the channel film of 100 nm . The lateral growth happens when the film is fully melted. Also, due to the Gaussian profile, the cooling rate is much smaller than conventional ELA technique with pulsed beam profile. The lateral growth region in our system sustain for a large laser energy window. The appearance of fine grain region is directly related to the cooling rate, while the cooling rate is controlled by the laser energy and the scan pitch. When the scan pitch increases, the cooling rate increases rapidly and the fine grain region starts to appear on the crystallized Si film, as shown in figure 2-3, when the laser energy density after the 645 mJ/cm^2 , fine grain region was formed.

2-3-2. Light absorptivity of different film

The critical energy, E_c , is associated with the absorptivity of the a-Si film. Since the penetration depth of 532-nm-wavelength laser into a-Si film is larger than 70 nm. The beam reflects from the bottom interface of the a-Si film will interfere with the incident laser beam. As a result, the absorptivity is found to be strongly related to the film thickness. According to previous report [17], the absorptivity of 532-nm-wavelength laser reaches peak value when the film thickness is around 50-60 nm. Compared with the E_c in our experiment, excellent agreement is observed. The critical energy is lowest when the film thickness is around 50-60 nm.

2-4. Device characterization

2-4-1. Process windows of Solid State Laser

Process windows of solid state laser were shown in figure 2-4-1(a). Unlike ELA laser crystallization, this Nd:YAG laser with Gaussian beam profile provides large process window for the super lateral growth (SLG) crystallization regime on a-Si thin film. The SLG process window can be defined between the critical energy density (E_c , the energy density that the grain starts to laterally grow) and the fine grain energy density (E_{fg} , the energy density that fine grain region starts to appear). For example, for devices with 50-nm active layer, their output characteristics become excellent while the active layer is annealed by laser with energy density from 484 mJ/cm^2 to 553 mJ/cm^2 and scan pitch as 2 μm . Within this process window, the device performance is good and uniform. With typical top-gate structure, the field effect mobility can be larger than 250 $cm^2/V.s$, and the threshold voltage can be lower than 1 V. More importantly, this process window for good device performance is consistent with the material analysis results.

2-4-2. Devices turn-on parameter

The devices turn-on parameter of different grain size and film quality is shown in table I . It shown the larger grain size, the well performance of field effect mobility, threshold voltage and subthreshold swing.

2-4-3. Devices turn-off characteristics

Transfer characteristics of different grain size and film quality was show in figure 2-4-3(a),2-4-3(b). In the off region, under low drain voltage as shown in figure2-4-3(a), off current unchanged. It shown that off current was independent of grain size, it may due to the leakage current mechanism of Thermionic emission, and the Mid-Gap trap density dominate. Under high drain voltage, I_{off} decreases when grain size increases. It may be due to the leakage current mechanism of thermionic field emission or pure field emission.

2-5. Grain Barrier Height Model

Equation (2-5-1) is the well-know grain boundary barrier height model proposed firstly by Seto et al [11]. E_B represents the grain boundary barrier energy in above-threshold region. N_T represents the effective grain boundary trap density and n is the gate-induced carrier density. When there is no other temperature-sensitive mechanism, the measured activation energy could be served as the grain boundary energy barrier.

$$E_B = \frac{qN_T^2}{8\epsilon n} \quad (2-5-1)$$

When drain voltage is high, it has been proposed that the drain-induced grain barrier lowering (DIGBL) effect would influence carrier transport seriously [9,12, 13]. When

the device is operated in the linear region and the drain voltage is low, the barrier increases with increasing drain voltage. This can be explained by the influence of drain bias on the surface potential along the channel [15]. The average carrier density is therefore expressed as [16]:

$$n = \frac{C_{ox}(V_G - V_{fb} - \alpha V_D)}{qt_{ch}} \quad (2-5-2)$$

where C_{ox} is capacitance per unit area, V_{fb} is the flatband voltage, and α is a parameter indicating the influence of drain voltage. t_{ch} is the channel thickness. According to the grain boundary barrier height given by Ref. [14], the barrier height considering the influence of the drain voltage and the DIGBL effect is given by

$$E_B = \frac{t_{ch}[(qN_T)^2 - 4qN_T\epsilon_s\eta\frac{V_D}{L}]}{8\epsilon_s C_{ox}(V_G - V_T - \alpha V_{DSe})} \quad (2-5-3)$$

For MOSFET devices, the channel thickness is reversely proportional to the gate bias and can be expressed as Ref. [9]:

$$t_{ch} = 8 \frac{V_{th}}{V_G - V_T} t_{ox} \sqrt{\frac{\epsilon_s}{\epsilon_{ox}}} \quad (2-5-4)$$

Where t_{ox} is the oxide thickness and V_{th} is thermal voltage. However, in poly-Si TFTs, the channel thickness would be further affected by the screening effect of trapped charges. So we modified the channel thickness as:

$$t_{ch} = 8 \left(\frac{V_{th}}{V_G - V_t} \right)^{\gamma-1} t_{ox} \sqrt{\frac{\epsilon_s}{\epsilon_{ox}}} \quad (2-5-5)$$

where γ is the parameter that represents the trapped charge screening effect. Finally, grain barrier height model of polysilicon TFT is expressed as:

$$E_B = \frac{t_{ox}V_{th} \left(q^2N_T^2 - 4qN_T\epsilon_s\eta\frac{V_D}{L} \right)}{\sqrt{\epsilon_{ox}\epsilon_s} C_{ox}(V_G - V_T - \alpha V_{DSe})^\gamma} \quad [22]$$

2-6. Activation Energy Analysis

Activation energy extraction is that choosing a bias condition, and to measure the output current in many different environment temperature. The temperature dependence of the mobile electron in equilibrium with the trapped charge is given by

$$I = I_0 \exp\left(-\frac{E_B}{KT}\right)$$

I_0 =constant independent of temperature

E_B = drain current activation energy which measures the difference between the valence band edge and the energy of the grain boundary states within KT of the Fermi level.

In this method, E_B is obtained from the Arrhenius plot for the $\ln\left(\frac{I}{I_0}\right)$ versus $\left(\frac{1}{T}\right)$ plot.

The activation energy can be extracted from the slop of Arrhenius plot. After changing the different bias condition, the activation energy versus the gate voltage plot can be generated. It's seen in figure 2-5-1.

It should be noted that there is a strong scattering effect when the devices are measured at high gate voltage and high temperatures. When the film quality was good, the scatter mechanism disappear faster at a small gate voltage. It should be careful not to include these data into the extraction of grain barrier height.

The curves of E_B versus V_G and $1/E_B$ versus V_G for devices with different film properties are shown in Fig 2-5-2, where the inverse grain barrier height of solid state laser which the grain size about $0.55(\mu m)$ is linearly proportional to the gate voltage. This indicates that the trapped charge screening effect is serious and the channel thickness keeps constant and is not dependent on gate voltage ($\gamma=1$), and it is also know the solid phase crystallization(SPC) and as deposited poly-Si is also have the γ value equal to 1[22]. Table II lists γ value for different grain growth conditions.

It is well-known that, when drain electric increases, the dominant leakage current

mechanism changes from thermionic emission, thermionic field emission, to pure tunneling [23]. At a low drain field (0.1V), the lowest activation energy is 0.46 eV. Since the E_B is about $Eg/2$, thermionic emission is the dominant leakage current mechanism at low field. As the drain bias increases, the drain depletion field increases and E_B decrease. This suggest that the high field in the drain depletion region has reduced the barrier that carrier must overcome. As much, the dominant leakage current mechanism is thermionic field emission. This process could be accomplished by combination of emission and tunneling processes. Further increase of the drain bias, there are almost no barrier to the carrier motion, so the dominant leakage mechanism is pure tunneling.

The activation energy of different grain size was shown in figure 2-5-3. it shows the same results as mention in section 2-4-3, under low drain voltage, I_{off} unchanged. It can be seen that I_{off} current was independent of grain size. Under high drain voltage, I_{off} decreases when grain size increases. The turn on region is defined as the activation energy achieving a specific small value which is negligible as shown in figure 2-5-4. Therefore, the devices fabricated by SSL turn on faster than ELA devices.

2-7 Trap State Density Analysis

By the extract of trap state density, effective trap state density can be obtained from the slope of the curve $\ln[I_D/(V_G-V_t)]$ versus $(V_G-V_t)^{-2}$ as shown in figure 2-5-5. The smaller grain size will involve the large amount of defects serving as trap states locate in the disordered grain boundary regions as shown in figure 2-5-6. As the grain size is decrease, the trap state density will increase.

Chapter 3

Characteristics of photo leakage current of Poly-Si TFTs

3-1. Optical absorption

The photon energy will be absorbed by the silicon film to excite the generation of electron-hole pairs. Under certain electric field such as the built-in electric field in the depletion regions, the electron and the hole will move toward the opposite direction and form the current. Compared to the generation current from the depletion region in the dark environment, this light-caused current is much larger and causes pronounced leakage current issues. And the optical absorption was introduced as blow:

Photon energy was defined as

$$E = hv = \frac{hc}{\lambda} = \frac{1.24}{\lambda} \mu m$$

Where h is Plank's constant and v is frequency

There are several possible photon-semiconductor interaction mechanisms. For instance, photons can interact with the semiconductor lattice whereby the photon energy is converted into heat. Photons can interact with impurity atoms, such as donors or acceptors, or they can interact with defects within the semiconductor.

If the photon energy is less than E_g , the photons are not readily absorbed, the light is transmitted through the material and the semiconductor appears to be transparent.

When a semiconductor is illuminated from a light source with hv greater than E_g and the intensity of the photon flux is denoted by $I(x)$ and is expressed in terms of

energy/cm². Figure 3-1 shows an incident photon intensity at a position x and the photon flux emerging at a distance $x + dx$. The energy absorbed per unit time in the distance dx is given by $\alpha I(x)dx$, where α is the absorption coefficient, given in units of cm^{-1} from the figure, we can write

$$I(x + dx) - I(x) = \frac{dI(x)}{dx} dx = -\alpha I(x) dx \quad (3-1-1)$$

If the initial condition is given as $I(x = 0) = I_0$

Above equation can be rewritten as follow:

$$I(x) = I_0 e^{-\alpha x} \quad (3-1-2)$$

Equation 3-1-2 represents the intensity of the photon flux decreases exponentially with distance through the semiconductor material

3-2. Photo leakage current

Polycrystalline silicon is much less sensitive to light than amorphous silicon, when Poly-Si TFTs are applied to display projectors which light luminance was above 5000 cd/m^2 , optical energy induced the carrier transform which caused the photo leakage current couldn't be ignored. Figure 3-2 shows the characteristics of drain current with various illumination of poly-Si TFTs, the light of scattering or direct illuminated pass through the active layer of poly-Si TFT, and the channel edge of depletion region was stimulated to generate electron-hole pairs. The photon can interact with a valence electron and elevate the electron into the conduction band. These electrons can diffuse easily and not control by the potential barrier, and move to the reverse bias of the electric field direction, hole carriers pass through the channel and electrons pass through the drain side, causing the photo leakage current.

The photo leakage current was defined by

$$I_{photo} = I_{illumination} - I_{dark}$$

The photo leakage currents of hydrogenated devices had certain characteristic features such as channel length independence and a weak gate bias dependence. In figure 3-3 and figure 3-4, the weak gate bias shows that there is no electric field enhanced component to the photon induced generation rate, in contrast to the field enhancement of the dark current [19]. And it may be caused by the weak drain voltage due to the various depletion region [20].

The dependence of photo leakage current on channel width (W) and channel length (L) are shown in figure 3-5 and 3-6. Photo leakage current is proportional to the channel width; however it is not strongly dependent on channel length. It might be because the photo current is generated from the depletion region near the drain side. So we could find the higher photo current in the wider channel width, the larger photo leakage current would obtain.

The photo leakage current of various LDD length was shown in figure 3-7. The higher LDD length, the larger photo leakage current will be generated. At the same time, as the LDD length increase, lateral electric field will decrease, the dark current will decrease. And the design rule was LDD length between 1-2 μm can suppress the photo leakage current as well as dark current.

It is well known the smaller grain size will involve the large amount of defects serving as trap states located in the disordered grain boundary regions. Polysilicon TFTs after a 10-min hydrogenation device was used to discuss the grain size effect versus trap state density (cm^{-2}) and photo leakage current. The results are summarized in figure 3-8. It is found that photo leakage current increases when the grain size becomes smaller. Since the grain boundaries are believed to be more amorphous-like crystal structure, they should have better absorptivity than the area

inside the grain. As a result, when grain size becomes smaller, the portion of grain boundaries becomes larger in a unit volume of silicon film. The photo leakage current is therefore increased.

The various channel thickness of same grain size was shown in figure 3-9, as the channel thickness increased, the photo leakage current would increase, it was due to the larger absorptivity and the wider depletion region.

3-3. Photo leakage current of poly-Si TFTs with illumination of RGB color

Recently, improvement of Lm/W for high-power RGB-LEDs allows large size applications with LED backlight in place of the conventional Cold Cathode Fluorescent Lamp (CCFL). When the color sequential technology is used to generate white color with color coordinate (0.3335,0.3331). The color coordinate of RGB-LED is (0.686,0.309), (0.28,0.675), (0.14,0.06) respectively as shown in figure3-10. And the spectrum of RGB colors was shown in figure3-11. The color coordinate of RGB-LEDs applied to the color sequential with the radiant flux of white color coordinate will be calculated from appendix XIII [25], the value in table IV shows the radiant flux intensity(Watt) of RGB colors have almost st same value.

Optical spectrum of CCFL back light was measured by the spectrometer, the wavelength of CCFL backlight was shown in figure 3-12. In our experiment, we try to produce the RGB light sources by using simple filtering films on the CCFL backlight system. And the optical spectrum of CCFL back light utilizing the simple filter of RGB sources was shown in figure 3-13. The color coordinate(x,y) of R、G、B color was shown in figure3-14, the value of R、G、B color coordinate(x,y) was (0.66,0.32)、(0.15,0.08)、(0.32,0.58) respectively.

In order to discuss the photo leakage current with illumination of the RGB color. In our experimental, the light of RGB color was illuminated with the radiant flux of 0.47 ($mWatt/cm^2$). Figure 3-15 shows the photo leakage current of various grain sizes under the illumination of RGB color. It obtains an interesting result about the largest photo leakage current with the illumination of blue color. We think the largest photo leakage current with the illumination of blue color may due to the largest absorptivity.

3-4 Optical properties of poly-Si film

In this section, absorptivity of different film was calculated. The optical constants, refractive index(n)and extinction coefficient (k) were measured by the n&k analyzer1280, and the value of n and k was shown in figure 3-16and 3-17. The optical absorption coefficients was determined by [24]

$$\alpha = \frac{4\pi k}{\lambda} \quad (3-1)$$

For comparison the corresponding sets of $n(\lambda)$ and $k(\lambda)$ for c-Si and a-Si in the same wavelength region are also plotted in Fig.3-18. The optical data for c-Si and a-Si are taken from the handbook of optical constants of Solids. [18]

The value of n and k can determine the absorptance coefficient, and then the absorptivity was determined by the reflectance and absorptance coefficient and then derived from the Beer's law[24]:

$$A = (1 - R)(1 - \exp^{-\alpha x}) \quad (3-2)$$

Where R is reflectance and x is thickness.

At the same time, absorptivity with the various grain sizes in the channel thickness of 50 nm was shown in figure3-19. As grain size decrease, it shows the larger absorptivity as we used the color of RGB illumination. It also agreements as mention above, as the grain size decrease, photo leakage current increase, and illumination of

blue color has the larger photo leakage current because of larger absorptivity.

The absorptivity of different poly-Si thickness derived from the equation 3-2 was shown in figure 3-20. It was also investigate the absorptivity with different poly-Si thickness as shown in Figure 3-21. [17]

3-5 Simulation of photo number per second with the illumination of RGB color into the poly-Si film

In order to discuss influenced of the photo leakage current with the illumination of RGB color, Table V shows the influenced of the illumination of RGB color. The absorptivity of different RGB color seems not to explain the influenced of photo leakage current with the illumination of RGB color. So we conclude the influenced was due to the optical energy and the absorption photo number. And assumption the photo leakage current is proportional to the photon number, so the photo number is calculated as follow:

The energy absorbed per second is

$$I' = (1 - R)I_0$$

$$I = I'(1 - \exp^{-\alpha x})$$

Photons can interact with the semiconductor lattice whereby the photon energy is converted into heat.

If the photon energy is greater than E_g , an electron-hole pair is generated and, in addition, the excess energy ($h\nu - E_g$) is dissipated as heat.

The portion of each photon's energy that is converted to heat

$$H\% = \frac{h\nu - E_g}{h\nu} \times 100\%$$

Therefore, the amount of energy dissipated per second to the lattice is

$$I_L = I \times H\%$$

The recombination radiation accounts

$$I_T = I_L - I$$

The number of photons per second from recombination is

$$\frac{I_T}{\text{Material Band Gap Energy}} (\# \text{ photon/s})$$

The photon number with different grain size under the simulation was shown in figure 3-22 and 3-23, it is agreement with the results of photo leakage current compare with the simulate photon number per second. It also shows the different crystalline quality of ELA as shown in figure 3-24. Therefore, the photo leakage current under the illumination of RGB color has the same trend compared with the photon number. The simulation result shows the photo leakage current was determinate by the absorption photon number and optical energy ($h\nu$). From the curve of the photo leakage current with the illumination of RGB colors. Photo current is determined by the absorptive photon number per second. The light of blue color has the largest photo current because color of blue light has the largest photon number per second.

Chapter 4

Conclusion

In this thesis, photo leakage current in typical top-gated poly-Si TFTs is studied. The dependences of photo leakage current on the channel width, the channel length, the lightly-doped drain (LDD) length, the grain size and the channel thickness are characterized. Photo leakage current is proportional to channel width and LDD length; however it is not dependent on channel length. This is because the photo current is generated from the depletion region near the drain side. As a result, increase the channel width or increase the LDD length can increase the depletion region and therefore enlarge the photo leakage current. In addition, the dependence of photo leakage current on the channel thickness is also investigated. As the channel thickness increases, the photo leakage current increase. Since the generation of photo leakage current is proportional to the absorptivity, increasing channel thickness effectively enlarge the photo leakage current. Also, the grain size influence on the photo leakage current is also investigated. It is found that photo leakage current increases when the grain size becomes smaller. Since the grain boundaries are believed to be more amorphous-like crystal structure, they should have better absorptivity than the area inside the grain. As a result, when grain size becomes smaller, the portion of grain boundaries becomes larger in a unit volume of silicon film. The photo leakage current is therefore increased.

Finally, in order to investigate the influence of photo leakage with illumination of RGB color, we try to produce the RGB light sources by using simple filtering films on the CCFL backlight system. It is found that under identical luminance, blue light is much more effective to generate photo leakage current. Also, if the color sequential is

designed to produce the white light with color coordinate (0.3335, 0.3331), blue light also generate largest leakage current. The leakage current in the blue light shining period is more than one order larger than those in red or in green light shining period.

The variance of the photo leakage current under different light sources is well explained by consider both the photon number per second and the optical energy ($h\nu$). Good agreement is found between the calculated data and the measured results.



Reference

- [1] D.Pribat, P. Leganeus, F. Plais, C. Reita, F. Petinot, and O.Hurt. "low temparture polysilicon material and devices", Inproc. Mater. Res. Soc.Vol.424,1997,pp.127.
- [2] S. D. Brotherton, "Topical review: polycrystalline silicon thin-film transistors", *Semicon. Sci. Technol*,Vol.10, pp.721-738, 1995.
- [3] Akito Hara*, Fumiyo Takeuchi, Michiko Takei, Katsuyuki Suga, Kenichi Yoshino, Mitsuru Chida, Yasuyuki Sano and Nobuo Sasaki " High-Performance Polycrystalline Silicon Thin Film Transistors on Non-Alkali Glass Produced Using Continuous Wave Laser Lateral Crystallization", *Jpn. J. Appl. Phys. Vol. 41* (2002) L311-L313.
- [4] Yutaka Nanno,el, at"Analysis of Photocurrents in Low-Temperature Polysilicon Thin-Film Transistors and the Use of Simulation to Design LDD Devices", *Electronics and Communications in Japan, Part 2, Vol. 86, No. 11, 2003.*
- [5] Kazuhiro Kobayashi et " Photo-leakage current of poly-Si thin film transistor with offset and lightly doped drain structure" *Jpn. J. Appl. Phys., Vol.38* (1999) pp.5757-5761.
- [6] S. D. Brotherton, J. R. Ayres, and N. D. Young "Characterization of low temperature poly-Si thin film transistors" , *solid-state electron*, Vol.34,pp.1991.
- [7] D. N. Yaung, Y. K. Fang, C. H .Chen, C. C. Hung, F. C. Tsao, S. G. Wu, and M. S. Liang, "to suppress photoexcited current of hydrogenated polysilicon TFTs with low temperature oxidation of polychannel" , *IEEE electron device letters*,Vol.22, NO.1, 2001.
- [8] Y. Tomihari," Low Temperature Poly-Si TFT Liquid Crystal Light Valve (LCLV) with a Novel Light-Shielding Structure for High Performance Projection Displays" et al 2004 SID.
- [9] J. Levinson, F. R. Shepherd, P. J. Scanlon, W. D. Westwood, G. Este, and M. Rider, "Conductivity behavior in polycrystalline semiconductor thin film transistors," *J. Appl. Phys. Vol. 53*, pp.1193-1202, 1982.
- [10] Proano,R.E. Misage, R.S.Ast,D.G," Development and electrical properties of undoped polycrystalline silicon thin-film transistors", *Electron Devices, IEEE Transactions on*, Vol. 36, Issue 9,Part 2, Sept.1989 pp.1915-1922.
- [11] J. Y. Seto, "The electrical properties of polycrystalline silicon films," *J. Appl. Physics*, 46, 5247, (1975).
- [12] P. S. Lin, Jwin-Yen Guo and Ching-Yuan Wu,"A quasi-two-dimensional Analytical model for the turn-on characteristics of polysilicon thin-film transistors," *IEEE Trans. Electron Devices*, Vol. 37, No. 3, March 1990.

- [13] H. L. Chen and Ching-Yuan Wu, "A New I-V Model Considering the Impact-Ionization Effect Initiated by the DIGBL Current for the Intrinsic n-Channel Poly-Si TFT's," IEEE Trans. Electron Devices, Vol. 46, No. 4, April 1999.
- [14] Gi-Young Yang; Sung-Hoi Hur; Choong-Ki Kim; Chul-Hi Han, "A physical-Based Analytical Turn-On Model of Polysilicon Thin Film Transistors for Circuit Simulation", IEDM, pp.953-956 1995.
- [15] H. W. Zan, T. C. Chang, P. S. Shin, D. Z. Peng, T. Y. Huang, and C. Y. Chang, "Analysis of narrow width effects in polycrystalline silicon Thin Film Transistors.
- [16] N.Beck, J. Merier, Fric, Z. Remes, A. Poruba, R. Flukiger, J. Pohl, A. Shan, M Vanecek, "enhanced optical absorption in microcrystalline silicon", Journal of non-crystalline solids,198-200(1996).
- [17] United states patent Dec.9,2004, No 0248347 A1,"laser beam irradiation method and method of manufacturing a thin film transistor".
- [18] E. D. Palik : Handbook of Optical Constants of Solids (Academic Press, Orlando, 1985) p.457.
- [19] J. R. Ayres, S. D. Brotherton, I. R. Clarence, P. J. Dobson, "Photocurrents in poly-Si TFTs",IEE proc.-circuits devices syst.,vol.141,no.1february 1994
- [20] Thesis of an empirical leakage current model of polysilicon TFTs,p27
- [21] K. R. Olasupo, and M. K. Hatalis, "Leakage Current Mechanism in Sub-Micron Polysilicon Thin-Film Transistors," IEEE Trans.Electron Devices, Vol.43, No.8, 1996.
- [22] Chao-Chian Chiu, Master.Sci.Eng.,National Chiao Tung University, 2005 "Thesis of The analysis of grain boundary barrier effect in polycrystalline silicon."
- [23] IEEE Trans.on Electro.Devices, Vol.43.1996,pp.1218
- [24] A . Poruba, " Optical absorption and light scattering in microcrystalline silicon films and solar cells",JAP, Vol.88,2000.
- [25] 戴亞翔, "TFT-LCD 面板的驅動與設計", 五南書局, p12